Global Twisting Motion of Single Molecular KcsA Potassium Channel Upon Gating

Hirofumi Shimizu[1,2], Masayuki Iwamoto[1,2], Takashi Konno[1,2], Amiko Nihei[4], Yuji C. Sasaki[1,3] & Shigetoshi Oiki[1,2,*]

[1]CREST Sasaki-team, Japan Science and Technology Corporation, Tachikawa, Tokyo 190-0012, Japan, [2]Department of Molecular Physiology and Biophysics, University of Fukui Faculty of Medical Sciences, Fukui 910-1193, Japan, [3]Japan Synchrotron Radiation Research Institute, SPring-8, Sayo, Hyogo 679-5198, Japan, [4]Engineering Group, SII NanoTechnology Inc., Chiba 270-2222, Japan.
*Correspondence: oiki-fki@umin.ac.jp

Summary

Ion channels are signal transduction molecules that switch ion permeation pathways on and off (gating). Crystal structures of several kinds of potassium channels have revealed open and closed conformations, which provide static pictures of gating status. Here we studied KcsA potassium channels undergoing conformational changes at the single-molecule level. A KcsA channel with a gold nanocrystal attached was irradiated by white X-rays and motions of the diffraction spot from the nanocrystal were tracked in real-time. Upon gating, the KcsA channels twisted around the axis of the pore. These conformational changes were prevented by an open-channel blocker, tetrabuthylammonium. Random clockwise and counter-clockwise twisting in the range of several tens of degrees originated in the transmembrane domain, and was transmitted to the cytoplasmic domain. This coupling suggests a mechanical interplay between the transmembrane and cytoplasmic domains.

Introduction

The cell membrane is endowed with sensor molecules which transduce environmental changes into signaling pathways. Ion channels are signal transduction molecules, which sense chemical and physical stimuli; this leads to opening and closing of the channels which changes the membrane currents (Hille, 2001). Recently, the crystal structures of several kinds of potassium channels have been elucidated, including the pH-sensitive, Ca^{2+}-sensitive and voltage-sensitive channels (Doyle et al., 1998; Jiang et al., 2002; Jiang et al., 2003; Kuo et al., 2003; Long et al., 2005). The sensing parts of these molecules differ, but they have a canonical structure for ion-selective permeation

pore. The crystal structures of these channels presented the pore structure in different gating states: some of them closed and others in the open state. From these structures it has been suggested that potassium channels have common conformations for open and closed states and that the conformational changes between these two states follow a shared route. Recent studies have elucidated local changes in structure around the gating helix (inner helix or M2 helix) (Liu et al., 2001; Kelly and Gross, 2003; Webster et al., 2004). In homo-tetrameric potassium channels the helices from each subunit might exhibit concerted motions during conformational changes. However, these global changes have not been detected. Here we address the following questions: What is the global conformational change upon gating? How are the motions of the transmembrane and cytoplasmic domains coupled upon gating? Where is the origin of gating movements? We used the diffracted X-ray tracking (DXT) method to examine these issues (Sasaki et al., 2000; Sasaki et al., 2001; Okumura et al., 2004). A gold nanocrystal with an average size of 20-25 nm was attached to a channel molecule and irradiated with white X-rays. The diffraction spot from a single nanocrystal was traced at video rate and the trace locations were translated into movements in real space. Thus, th motions of the nanocrystal report the conformational changes of a single channel molecule. The data revealed the dynamic motions of channel molecules in different conformational states.

Results

Observation of KcsA channel from a fixed point of view
The KcsA channel (Schrempf et al., 1995; Heginbotham et al., 1999; LeMasurier et al., 2001) is the first potassium channel whose crystal structure has been examined at high-resolution (Doyle et al.,

1998; Zhou et al., 2001b). The possible changes in the structure upon gating have been predicted (Perozo et al., 1999; Kelly and Gross, 2003; Zimmer et al., 2006; Iwamoto et al., 2006). KcsA channels are gated when the cytoplasmic pH is acidic (Heginbotham et al., 1999). This property was exploited in our experiments in which different pHs were used to produce changes in the dynamic structure.

To observe conformational changes from a fixed view-point, the KcsA channels were attached to a flat glass surface (Fig. 1A). Channels with four symmetrical lysine-mutated sites (R52K and with other lysine residues mutated to arginine; see Methods for details.) were reacted with a modified glass surface, which secured the channel in an upright position. The orientation of the channels on the surface was confirmed by atomic force microscopy (AFM, Fig. 1B). The height of the fixed molecule from the flat surface was 9.9 nm (Fig. S1), which corresponds to the length of the KcsA channel (Cortes et al., 2001; Zimmer et al., 2006). This supports the idea that the channel was in an upright orientation at a slight slant angle (Fig. S2). A one-dimensional gold nanocrystal (Fig. S3) was attached to the KcsA channel through cysteine residues introduced at the end of the C-terminus. This site (161C) is located at the end of the molecule and is the most exposed site on the surface of the molecule (Iwamoto et al., 2006). The four cysteine residues in the tetrameric channel hold the nanocrystal. Thus, the channel was oriented with one end attached to the flat quartz surface through its extracellular loops and the other end free in the solution phase with the gold nanocrystal attached. The mutated KcsA channel reconstituted into a planar lipid bilayer showed gating activity at acidic pH (Iwamoto et al., 2006). Gold-labeling of the channel modified its gating properties only slightly (Fig.
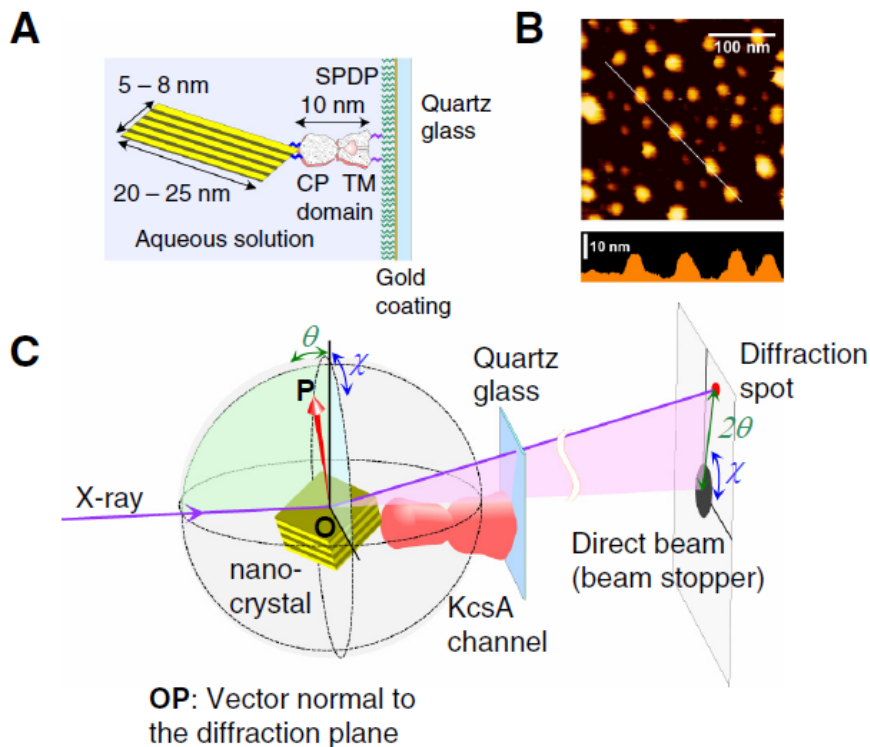
Figure 1. DXT measurements of a gold-labeled KcsA channel. **A.** KcsA channel fixed onto a glass plate. Mutated lysine residues (R52K; violet lines) in the extracellular loop of tetrameric channel were reacted with the LC-SPDP-modified surface (the length of the molecule: 1.6 nm). A nanocrystal was attached to the C-terminal end (161C; blue lines) of KcsA channel. The TM and CP domains represent the transmembrane and cytoplasmic domains. **B.** The AFM image of KcsA channels in an aqueous solution. The lower panel shows the height profile scanned through the white line in the upper panel (see Supplemental data, Fig. S1).

C. Geometry of the DXT experiment showing the configuration of gold-labeled KcsA channel on the quartz glass in relation to the synchrotron radiation beam and the image plane (the right plate; positioned at 100 mm from the sample). Motion of the nanocrystal is defined as that of the vector normal to the diffraction plane (red arrow). Geometrical correlations between the movements of the vector in the real space and those of the spot on the image frame are shown. The center of the image frame was shadowed by the beam stopper and the outer limb of the observing frame was less than 20°. χ represents the rotational angle and θ represents the bending angle.

S4), indicating that labeled channels were functionally competent.

The principle of the DXT method is simple. The observation of diffraction spots from a crystal dates back to Laue's experiments using white X-rays (Friedrich et al., 1912). Shortly after that, Terada detected diffraction spots on a fluorescent plate and observed movements of the spots as the crystal was rotated (Terada, 1913a; 1913b; 1913c). These pioneer experiments in the early 20th century were refined to observe motions of single molecules. The crystal for diffraction was scaled down to a nanocrystal and high flux white X-rays from the synchrotron radiation facility (SPring-8) elicited observable diffraction spots from a single nanocrystal (Sasaki et al., 2001). The white spectra of X-rays enabled tracing of nanocrystal movements even if a nanocrystal changed its angle with respect to the beam. The beam shed on the crystal generated a single diffraction spot from the (200) crystal plane rather than multiple spots, because the structure of nanocrystals was one-dimensional (layer-by-layer; Okumura et al., 2005). With this method, the diffraction plane of a nanocrystal can be regarded as a tiny mirror. A spot diffracted from the "mirror" reports movements of nanocrystals through simple geometric rules (the Bragg reflection; Bragg and Bragg, 1913; Fig. 1C).

Pulse trains of white X-rays were irradiated normal to the glass surface or parallel to the longitudinal axis of the channel molecule (Fig. 1C). When the channel bends, the diffraction spot moves radially as defined by the angle θ. The range of the observable angle θ was 7° to 20°. When the channel rotates, the spot also rotates in the image plane with the angle χ. These χ and θ angles were defined for the movements of the crystal in real space.

KcsA channels without cysteine residues were attached to the plate and nanocrystals were added. This sample gave virtually no diffraction spots (7 spots out of 316 recording frames), indicating that the nanocrystal labeled only the cysteine site introduced into the channel.

Quiet KcsA channel with Brownian fluctuations
The KcsA channel remained closed when the pH of the solution was set at 7.5. On an image plane several spots were observed, each represented a diffraction spot from a different nanocrystal (Fig. 2A, left panel). The right panels show snapshots of images for diffraction spots (see the video file "Movie S1"). The movements of the spots were random and were independent of each other. Most of the trajectories of spots, superimposed on an image plane (Fig. 2B), showed radial movements (the θ angle). The polar coordinates of diffraction spots on the image plane were converted to the orthogonal axes (χ-θ coordinates) to see the crystal motions in real space (Fig 2C). The time courses of the crystal motions were plotted as changes in χ and θ with time (t). Most of the spots seemed to run parallel to the time axis, meaning that both rotational and bending motions were small. This was seen by projecting spots on the χ-θ plane (Fig. 2C lower). Rotational movements were rarely seen under this condition. Local movements of each spot are shown by setting the starting position of the spots at the origin of the χ-θ coordinate (Fig. 2D). Representative trajectories show that a bending motion was slightly preferred. This motion corresponds to the bending motion along the longitudinal axis of the channel, or a wobble motion. Spots rarely went out of the image frame and stayed in a restricted area throughout the recording time of 3.8 s. Continual movements throughout the recording period suggested that the channel proteins were rarely damaged by irradiation (Fig. S8). The channels were in a quiet state at pH 7.5 and these small movements represented thermal fluctuations of the channel (Sigg and Bezanilla, 2003; Sigg et al., 2003).

Active twisting motion upon gating
When the KcsA channel was in the active gating mode at pH 4.0, the trajectories of the diffraction spots changed dramatically (Fig. 2E). Significant circumferential movements were seen (Fig. 2F; see the video file "Movie S2" in supplemental data). These spot motions were translated into crystal motions in real space (Fig. 2G). Motions along the χ axis predominated and the trajectories were tangled with each other. These motions corresponded to rotational movements around the axis of the channel. This is the first observation of channel gating as a rotational motion. Clockwise and counter-clockwise rotations were observed, reflecting random opening and closing motions. There were also simultaneous increases in radial motions, so the spots exhibited complicated trajectories and covered a wide range of rotational angles. Most of the spots (321 rotating spots out of 489 spots) showed significant movements in the χ direction, Trajectories of several spots in χ-θ coordinates are seen in Fig. 2H, in which the starting positions were set to the origin of the coordinate. The rotational motions predominated and the ranges of the rotational movements far exceeded the bending movements. Spots often continued moving in the same rotational direction for several steps. This may be a sign of a deviation from random motion along the rotational axis. Hereafter this motion will be called twisting.
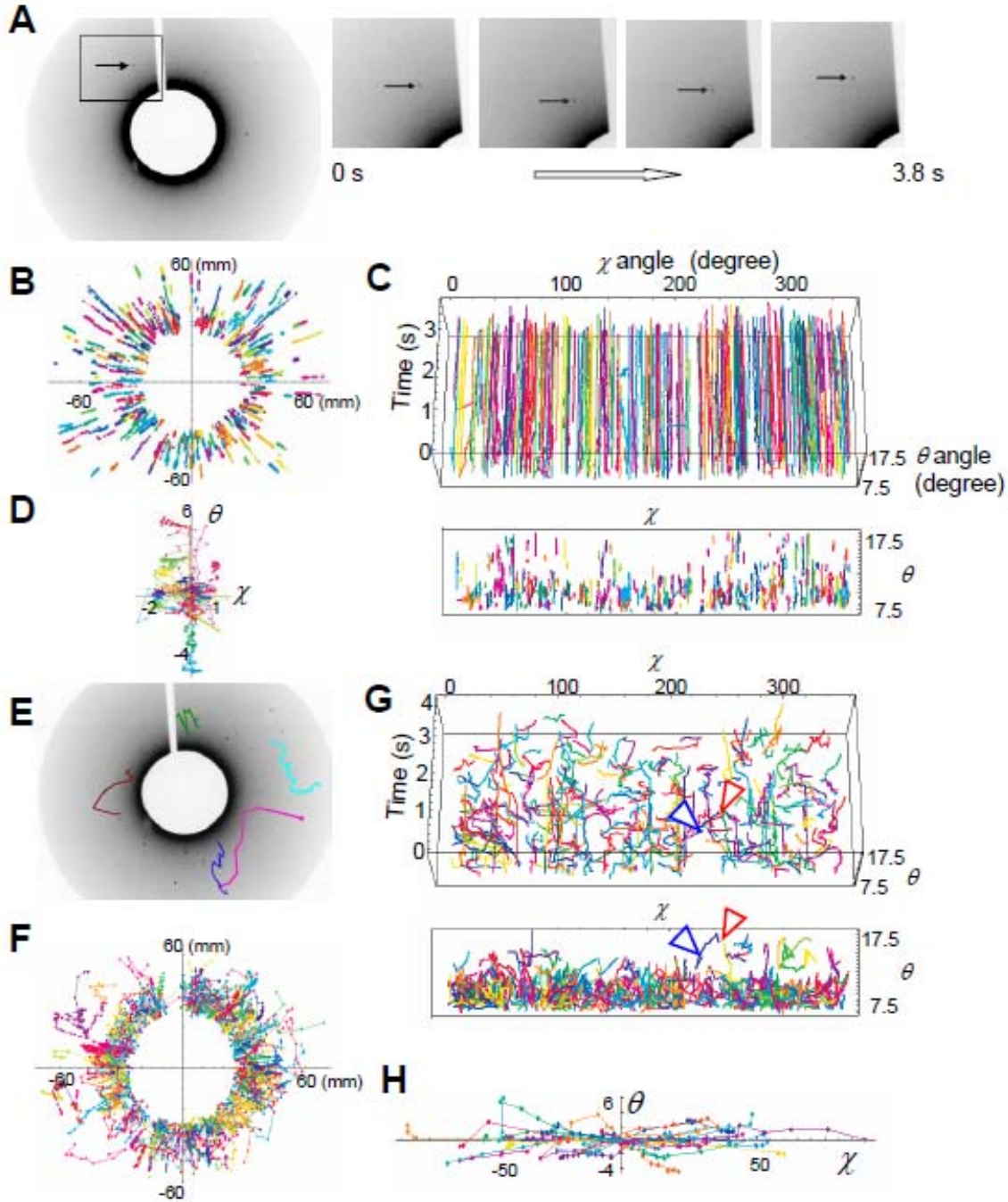
Figure 2. Motions of the diffraction spots in image frame and motions of the channels in real space. **A-D.** Movements of KcsA channel at pH 7.5. **A.** Images of diffraction spots. The reversal images are shown. **Left panel**. Diffraction spots on an image frame. In the frame the shadow of the beam stopper was projected at the center and the vertical bar. **Right panels**. Time series of image frames of diffraction spots. The rectangular area in the left panel was enlarged and a few images picked up (the interval of the images was 1.3 s) from a time series of video frames (30 frames/s) was shown.. Motions of a diffraction spot are indicated by arrows. **B.** Trajectories of diffraction spots on an image plane. Trajectories of spots are superimposed. The origin of the x-y coordinates (in mm scale) is the position to which direct beam projects.

4

Since the movements were so active, moving spots frequently strayed from the image frame during the 3.8 s recording period. One of these short-lived trajectories for channel motion in real space is labeled with arrow heads in Fig. 2G, in which a moving spot appeared spontaneously in the recording range [blue arrow head] and soon disappeared [red arrow head]. At the end of a short track, the spot may have taken a large step from the last observed position or gone out of the recording range of the image frame. On the other hand, some spots stopped moving after vigorous motion and never moved again. The brief dwell times of spots in the recording frame are shown as a histogram (Fig. 3A, red histogram). The lifetimes of the spots decayed exponentially with a time constant of 480 ms. This is in contrast to the lifetimes of the spots in the quiet state when most of the spots remained in a frame throughout the recording period (Fig. 3A blue).

The active movements were compared quantitatively with those during the quiet state using histograms of the displacements of the destination position relative to the initial position (Fig. 3B). In the quiet state, the distributions of the displacements for the χ and θ angles were Gaussian (blue). This indicates that the spots moved in random along the rotational and tilt axes and accumulations of random motions formed the Gaussian distribution. The widths of the distributions were small, indicating that the random motions were restricted. In contrast, the histogram for the χ angle during gating was distributed broadly in both rotational directions up to ±40 degrees. In this plot the positive coordinate of the χ angle represents clockwise twisting of the channel molecule viewed from the cytoplasmic side. The shapes of the χ distributions were irregular and non-Gaussian, suggesting a possibility that non-random perturbations were imposed on the motion. For the bend angle, the distributions of the histogram during

activation were broader than those of the quiet channel.

When the measurements were performed at temperatures below 15 °C, instead of at 18 °C, the frequency of twisting motions of active gating was decreased dramatically. Above 20 °C the movements of spots could not be followed due to the rapid skimming of spots on the image frame. The apparent high temperature dependence of the motion may originate partly from limited resolution for detecting fast moving spots, and may be accounted for by a high activation enthalpy for the conformational changes of the twisting gate.

Perspective of channel motion from different viewpoints

To reconstruct the channel motion in three-dimensional space, we fixed channels in different orientations and observed them from different points of view. The channels were first set in the erect position, the reverse of the orientation used previously: The C-terminal end of the cytoplasmic domain was fixed to the glass plate and the extracellular loop was gold labeled (161K-R52C, see Experimental Procedures). At pH 4.0 the twisting motions were similar to those of the upside-down channels (Fig. 4). This means that fixing the channel on a plate in either upright orientation (erect or upside-down) did not disrupt the channel function and that the twisting motions were transmitted along the longitudinal axis of the molecule.

Second, the channel was laid sideways: it was fixed at the middle of the N-terminal helix, which is located at the intracellular interface of the membrane (Fig. 4A, see Experimental Procedures). Viewing the channel in this orientation complements the limited information of motions observed through the narrow window for the θ angle. Surprisingly, the range of the spot motions in the χ direction was severely restricted

C. Trajectories of channel motions in real space in orthogonal t-χ-θ coordinates. Motions along the χ axis represent rotational motions and those along the θ axis represent tilt motions. **Upper panel.** The time courses of channel motions plotted as changes in χ and θ with time. The time scale is indicated from the time of the initial beam to the end of the recordings at 3.8 s. **Lower panel.** The trajectories were projected on the χ-θ coordinates. Note that the expansion of the scale of the θ angle. **D.** Displacement trajectories of channel motions from the initial position on χ-θ coordinates. Representative trajectories by setting the initial points at the origin of the χ-θ coordinates are shown. **E-H.** Active conformational changes of KcsA channel upon gating at pH 4.0. **E.** Representative trajectories of diffraction spots superimposed on an image frame. **F.** Trajectories of spots superimposed on an image plane. **G.** Trajectories of channel motions in the t-χ-θ coordinates. Blue and red arrow heads indicate starts and terminations of a trajectory. Spots appeared randomly in the time scale of recordings and disappeared spontaneously after short periods of active motion. In the lower panel, the trajectories were projected on the χ-θ coordinates. **H.** Displacement trajectories of channel motions upon gating from the initial position on χ-θ coordinates.
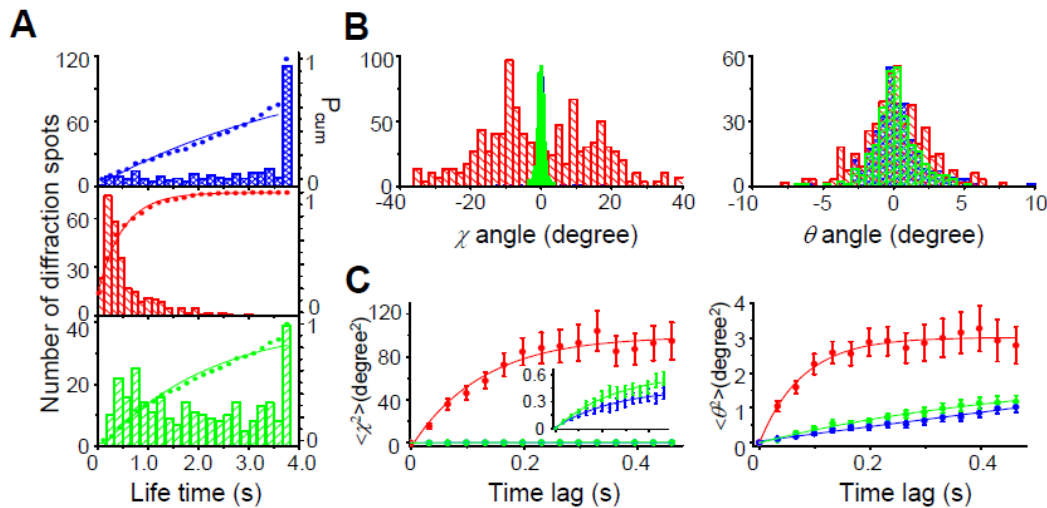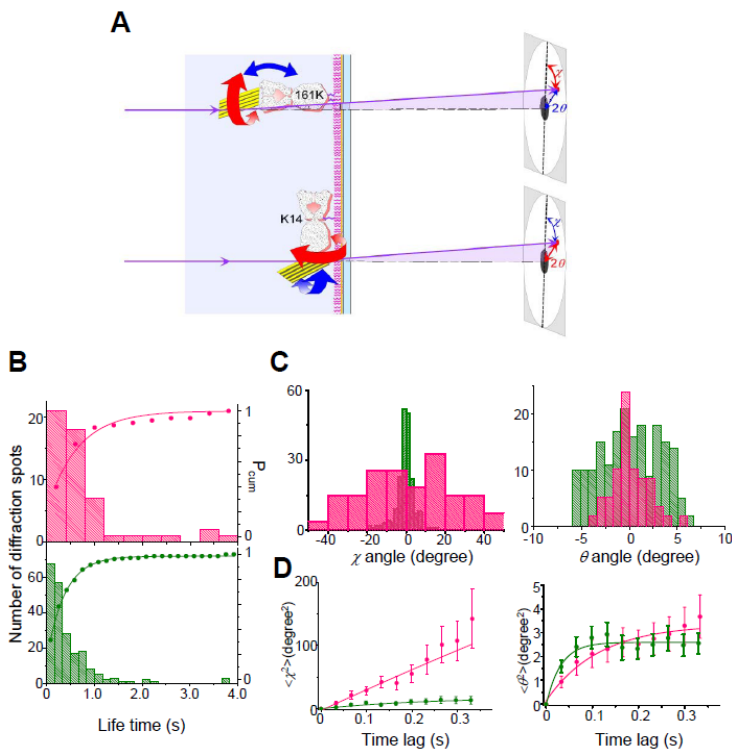
Figure 3. Motion statistics of KcsA channel in different states. Data for channels in the quiet state are shown in blue, the actively gated state in red and the blocked state in green.quiet (blue), actively gated (red) and blocked (green) states.

A. The lifetime of spots stayed in the frame during the 3.8 s recording time. Cumulative lifetimes were superimposed (dotted lines), from which the time constants were evaluated (4.33 s for the quiet, 479 ms for the actively gated and 2.04 s for the blocked channels). **B.** Distributions of the destination positions for χ and θ angles relative to the initial positions reached during the recording time. The vertical axis represents numbers of observations for the quiet channel and the scale of the axis was adjusted for the data of the actively gated and blocked states. The S.D. values of the distributions were 0.63° (pH7.5), 16.7° (pH4.0) and 0.74° (TBA) for the angle χ, and 1.2° (pH7.5), 2.1° (pH4.0) and 0.91° (TBA) for the angle θ. For actively gated channels, S.D. values were evaluated by assuming the distribution to be Gaussian. **C.** MSD curves. The range of the time lag was set to the time constant for the lifetime of spots at pH 4.0 (the middle of panel **A**). Diffusion coefficients derived from fitting the curves (see Experimental Procedures) were 0.83 degree^2/s (pH7.5), 417 degree^2/s (pH4.0) and 1.45 degree^2/s (TBA) for the angle χ, and 0.76 degree^2/s (pH7.5), 9.67 degree^2/s (pH4.0) and 1.02 degree^2/s (TBA) for the angle θ. Data are mean ± S.E.M. **Inset.** MSD curves for the angle χ with the vertical scale expanded.

for actively gated channels at pH 4.0 (Fig. 4C). In contrast, the motion in the θ direction became more vigorous. In this orientation the geometrical relationships between motions of a channel in real space and of a diffraction spot on the image plane became complicated. Motions of the χ angle involved bending motions but did not include twisting motions (Fig. 4A). On the other hand motions along the θ angle encompassed twisting motions as well as bending motions (Fig. S6). Therefore, the distributions of the destination angle for the χ axis represented the bending motion, which was fully traced in the absence of any restriction on the observing window. It should be noted that, compared to the nanocrystals on the upright channels, the nanocrystals on the channels laid sideways were placed close to the glass surface and may have bumped into the surface, leading to attenuated motion. The histograms of the destination angles for the θ direction were broader than those observed for the χ angle and those for the θ angle in the other orientations (Fig. 4C; Fig. S5), and both ends of the distribution were truncated. The results

suggest that this vigorous motion along the θ axis represented the twisting motion in this orientation, which led to the shortened lifetime (the time constant was 370 ms, Fig. 4B lower panel).

The reverse relationships of the spot motions in the χ and θ axes for the upright channels and the channels laid sideways seem to be the results of observing the motions from different viewpoints. Therefore, the underlying motions of channel molecules in real space may be conserved even if the patterns of the spot motions appeared to be different. The range of the bending motion was evaluated by using the data from the channels laid sideways, since the observation window for the χ angle was not restricted. The distributions of the bending motions were slightly broader than those observed for upright orientations, but were much narrower than those of the twisting motions. These results support the predominance of the twisting motions in active gating, regardless of the orientation of the channel molecules or the point of view.

Figure 4. Motion statistics of KcsA channels in different orientations. Data for channels in erect orientation are shown in red and laid orientation in green. **A.** A schematic representation of channel orientations (upper: erect; lower: laid sideways), their motions (red: twisting; blue: bending) and movements of the diffraction spots on the image plane. Erect channels were fixed at 161K and channels laid sideways were fixed at K14. The geometrical relationships between channel motions in real space and spot motions in image plane were nearly reversed for erect and sideways orientations. The bending motions of channels laid sideways also generated motions of diffraction spot along the θ axis. Compared to the upright orientations, the nanocrystal attached to channels laid sideways was located close to the glass surface. Conformational changes of channels may bump the nanocrystals onto the surface, which attenuated the range of motion. The size of the nanocrystal was not scaled relative to that of the channel.

B. The lifetime of spots stayed in the frame during the 3.8 s recording time. Cumulative lifetimes were superimposed (dotted lines). The time constants of the lifetime were 653 ms (erect channels) and 374 ms (sideways laid channels). **C.** Distributions of the destination positions for χ and θ angles relative to the initial positions reached during the recording time. The vertical axis represents numbers of observations for the quiet channel and the scale of the axis was adjusted for the data of the actively gated and blocked states. S.D. values of the distributions were 25.7° (erect channels) and 2.4° (sideways laid channels) for the angle χ, and 1.8° (erect channels) and 3.9° (channels laid sideways) for the angle θ. **D.** MSD curves. The left panel is for the angle χ and the right one for the angle θ. D values were 166 degree^2/s (erect channels) and 37 degree^2/s (sideways laid channels) for the angle χ, and 7.1 degree^2/s (erect channels) and 20.7 degree^2/s (channels laid sideways) for the angle θ. Data are mean ± S.E.M.

Dynamic properties of KcsA motions

To analyze the dynamic behavior of the motions, mean square displacement (MSD) curves, in which the squared displacement of spots from the initial position are displayed, were examined. MSD curves for the χ and θ angles (Sasaki et al., 2000) were drawn for the movements in the two pH conditions (Fig. 3C). In the quiet state at pH 7.5 an initial linear relationship followed by a slight sublinearity was seen for MSD curves of χ and . angles (blue symbols in the inset of the left panel and in the right panel), indicating that the channels were undergoing Brownian motion (Sasaki et al., 2000). The structure of the channel molecules fluctuated within a narrow range of a few degrees. The diffusion coefficients were evaluated from the linear parts of the MSD curves. In the quiet

state D_{bend} and D_{twist} values were similar (Fig. S5). No bias was posed in the direction of the fluctuations.

The MSD curves for the χ angle for channels during active gating at pH 4.0, showed dramatic increases in the initial slope followed by sub-linearity (red symbols). D_{twist} exceeded that at neutral pH by two orders-of-magnitude (Fig. S5). D_{bend} for the θ angle also increased. The channels were freer to twist upon gating.

MSD curves for the upright (erect and upside-down) orientations and the sideways orientation showed dramatic contrasts (Fig. 4D). D_{twist} and D_{bend} for the erect channels were similar to those of the upside-down channels (Fig. S5). In contrast the plot of the θ angle for the channels laid sideways showed a large initial slope followed by immediate saturation. This behavior reflects the presence of

vigorous twisting motions observed through the narrow window of the θ axis. On the other hand, for the χ angle, the MSD curve showed an attenuated slope and the distribution of the destinations was narrow. These results indicate that for the channels laid sideways the twisting motion along the χ axis was barely detectable.

The twisting motion upon gating had not been expected at the beginning of this experiment, because the nanocrystal was attached at the C-terminal end of
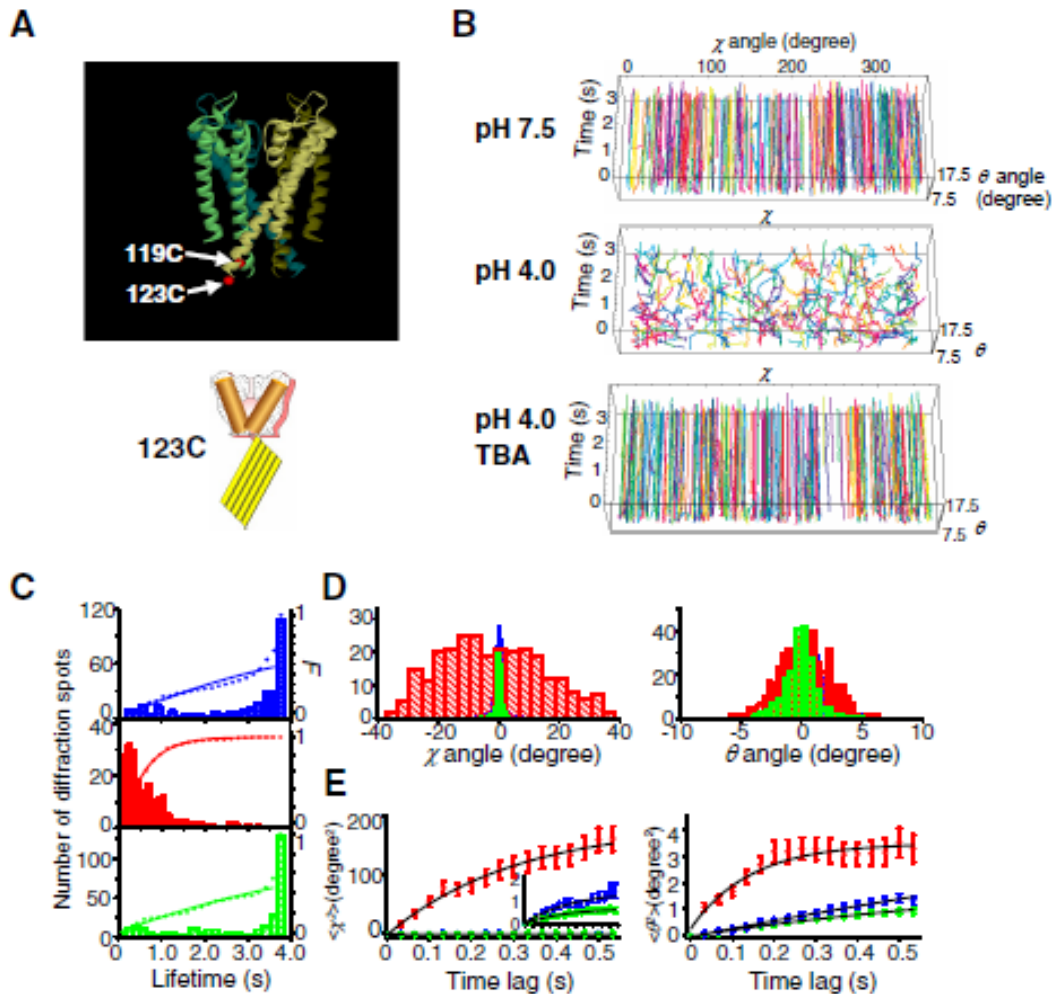
Figure 5. Motions of cytoplasmic domain-deleted KcsA channel. **A.** The structure of the CPD-deleted channel and labeling sites at the end of the M2 helix. **B.** Trajectories of channel motions in t-χ-θ coordinates at pH 7.5, at pH 4.0 without and with TBA. **C-E.** Motion statistics of CPD-deleted KcsA channel in quiet (blue), actively gated (red) and blocked (green) states. **C.** The lifetime of spots stayed in the frame during the 3.8 s recording time. Cumulative lifetimes were superimposed (dotted lines), from which the time constants were evaluated (5.36 s for the quiet, 527 ms for the actively gated and 5.94 s for the blocked channels). **D.** Distributions of the destination positions for χ and θ angles relative to the initial positions reached during the recording. The vertical axis represents numbers of observations for the quiet channel and the scale of the axis was adjusted for the data of the actively gated and blocked states. S.D. values of the distributions were 0.96° (pH7.5), 19.9° (pH4.0) and 0.62° (TBA) for the angle χ, and 1.46° (pH7.5), 2.2° (pH4.0) and 0.81° (TBA) for the angle θ. **E.** MSD curves for the angles χ and θ. D values were 2.29 degree^2/s (pH7.5), 311 degree^2/s (pH4.0) and 1.38 degree^2/s (TBA) for the angle χ, and 0.86 degree^2/s (pH7.5), 5.67 degree^2/s (pH4.0) and 0.66 degree^2/s (TBA) for the angle θ. Data are mean ± S.E.M. **Inset**. MSD curves for the angle χ with an expanded vertical scale.

the cytoplasmic domain, which was far (ca. 4 nm) from the transmembrane domain (TM domain, comprising of M1, M2 and P helices).

Cytoplasmic domain-deleted KcsA channel
To observe the gating movements directly, the cytoplasmic domain (CP domain) was deleted at the 125th residue (CPD-deleted channel) and the C-terminal end of the M2 helix was labeled with the nanocrystal (Fig. 5A).

When residue 123 was labeled, clear twisting motions were observed at low pH (Fig. 5B). Trajectories of spots in the t-χ-θ space revealed no twisting motion in the quiet state and vigorous twisting during active gating. The ranges of the histogram for destination position in the χ angle were ±40 degrees and the shapes were also irregular (Fig. 5D). The lifetimes of the spots were short but were prolonged significantly from that for the full-length channel (Fig. 5C; τ = 527 ms). The MSD curves were similar to those for full-length channels (Fig. 5E; Fig. S5).

When residue 119 was labeled there were no twisting motions at pH 4.0. The distributions of the destination positions were narrow (S.D. for the labeling at 119 was 0.91 ± 0.05 degree for the χ angle, and 0.32 ± 0.09 degree for the θ angle.). Our previous study revealed that site 119 was exposed to the surface of the molecule (Iwamoto et al., 2006), indicating secure labeling. Thus, it is suggested that labeling at this site may freeze the gating motion.

The existence of the twisting motion for the CPD-deleted KcsA channel suggests that the twisting motion originates from motions in the TM domain and that this is an authentic gating movement.

TBA blocking of gate movements
If the gating movement originates from the TM domain and transfers through the CP domain, what would happen if the gating were prevented by a channel blocker? Tetrabutylammonium (TBA) is an open channel blocker, and the structure of KcsA co-crystallized with TBA revealed that TBA blocks
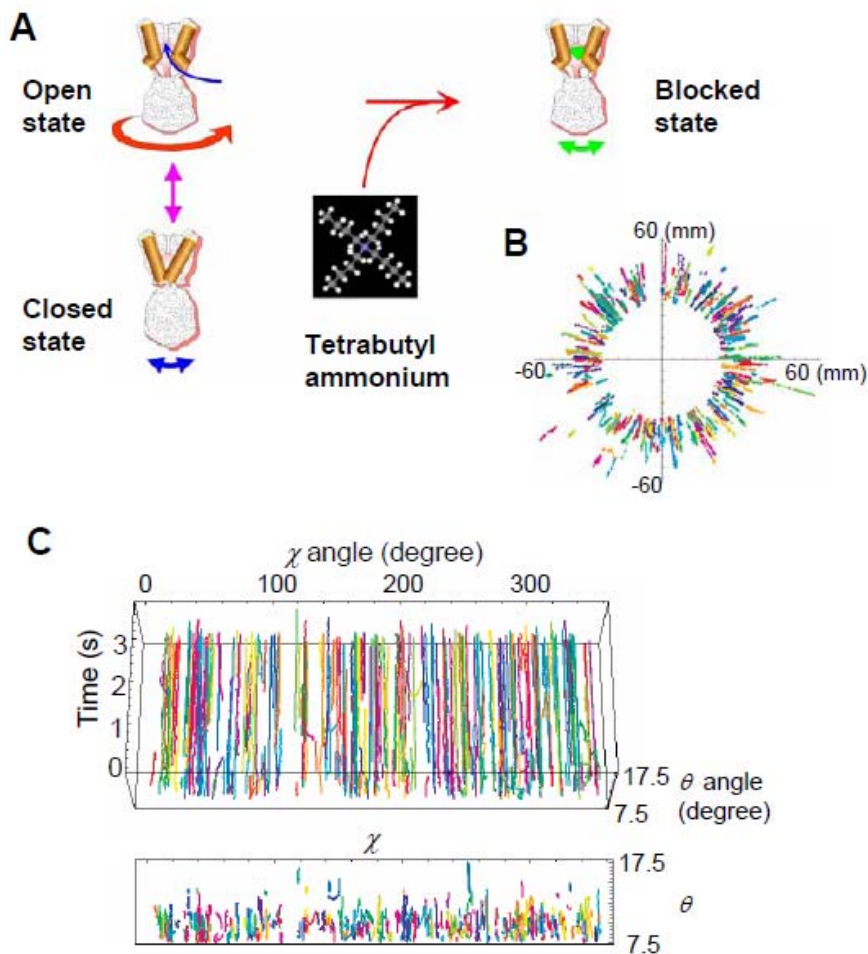
Figure 6. The blocking action of TBA on the intact KcsA channel. **A.** Schematic representation of open channel blocking by TBA. TBA settled in the central cavity where it blocked the current and kept the gate open at pH 4.0. **B.** Superimposed trajectories of spots on an image plane. **C.** Trajectories of channel motions in t-χ-θ coordinates.

9

within the central cavity (Faraldo-Gomez et al., 2007; Lenaeus et al., 2005; Zhou et al., 2001a). Also we have reported in a previous study that the gate was kept open by TBA in a channel that was otherwise gating actively at pH 4.0 (Fig. 6A; Iwamoto et al., 2006). DXT experiments were performed at pH 4.0 in the presence of 10 mM TBA for CPD-deleted and full-length KcsA channels. For the CPD-deleted channel, the twisting motion of KcsA was stopped completely (Fig. 5B lower panel). This also indicates that the twisting motion detected at pH 4.0 originates from the gating motion of the TM domain. The twisting motion of the full-length KcsA was also stopped by TBA (Fig. 6B, C). This suggests that the gating movements from the TM domain were transferred towards the end of the CP domain and that the CP domain was subject to passive rotation.

In our previous study (Iwamoto et al., 2006) we found that in the presence of TBA at pH 4.0 the residue 116 in the M2 helix became exposed on the surface of the molecule. This happens when the gating helix is bent in the open structure. The frozen behavior of spots observed by DXT under the TBA-blocked condition indicated that the channel rarely underwent conformational changes. Therefore the channel seems to be locked in the open state (open-locked state).

Discussion

In this study changes in the modes of the motions for the KcsA channel were detected by changing the experimental conditions (Fig. 7A). At neutral pH, where the channel was closed, motions along the bend axis were slightly preferred. Changing to an acidic pH, where the channel becomes actively gated, caused a twisting motion to appear. By adding TBA at low pH, the twisting motion stopped, and the channel became open-locked. Therefore, the motions observed under different experimental conditions represent motions in different conformational states: The closed state at pH 7.5, open-close transitions at pH 4.0 and the open-locked state in the presence of TBA at pH 4.0. These different modes of motions are represented quantitatively for the full-length and CPD-deleted channels (Fig. S5).

Motions of diffraction spots on the image plane were translated into motions of channel molecules in real space. During translation, the limited range of the detection window must be taken into considerations. For example, spots appeared spontaneously and escaped from the image frame during gating. If the motion was purely rotational, the spots should not disappear. Thus, one may consider that there should

be concomitant activation of the bending motion along with the twisting motion. However, with the DXT method, the sensitivity of detection of the motion along the θ axis is high but the covered recording range is limited. To estimate the degree of the bending motion, we observed motions of channels laid sideways (Fig. 4). In contrast to the vigorous motions along the θ angle (the twisting motion), we found that the distribution of motions for the χ angle (the bending motion) was limited. The latter motion reflects the real range of bending motions for the channels, since the observed range was not limited by the narrow window. The comparison of the range of bending motions for the channels laid sideways and upright channels revealed a slightly broader distribution for the former channels (Fig. 3B, 4C). This indicates that the narrow window of the θ angle altered the data describing the real bending motion to some extent, but the magnitude of cutoff was less than 15 % (Fig. S5A). If so why were the lifetimes short even with relatively small bending motions? It may be related to the orientations of the fixed channels on the plate. In the AFM images, the distributions of heights were not sharp (Fig. S1), suggesting some angle of slant in the channels fixed upright. If the directions of the beam and the axis of the channel were not parallel, the trajectories of spots for the pure rotational motions may become elliptical in the image plane. Thus, the superposition of the bending motions upon the twisting motion may have led to the escape of spots from the frame with short residence times, since the range of the radial motions in the image plane was augmented when the channel axis was slanted and the rotational trajectory approached apoapsis. The short residence times of spots seem to be the result of moderately activated bending motions and of the slant of the axis for the twisting motions.

The escape rates of the spots from the recording range can be estimated from the time constants of the lifetime (Fig. 3A and 5C). Faster escape rates for the full-length channels upon gating indicate that they exhibited more bending motion. This is supported by larger S.D.s of the Gaussian distributions and D values of the MSD curve for the θ angle (see Supplemental data, Fig. S5). It is likely that the CP domain imparts additional bending motions. This behavior is in agreement with our previous report that the CP domain becomes flexible during gating (Iwamoto et al., 2006). For the CPD-deleted channel in the TBA blocked state at pH 4.0, the spots stayed in the recording space throughout the recording time (Fig. 5B, C); this behavior is indistinguishable from that of the quiet state. In contrast, the spot lifetimes for full-length channels with TBA showed a significant

10

fraction of short-lived spots (Fig. 3A, and the estimated lifetime was 2.1 s). This also suggests that even if the gating helix is locked by TBA, the flexible CP domain at pH 4.0 bends relatively freely. In the absence of the twisting motion the diffraction spots stayed in the image frame for longer times and small bending motions accumulated and eventually the spot moved out of the recording frame.

It should also be noted that the observed ranges of motions along the χ axis may differ from the real range of twisting motions. Simulations of random motions of channels in different orientations and the resultant motions of diffraction spots gave estimates of the rotational angle as a function of slant angle (see Supplemental data, Fig. S6). The slant angle of the channel axis was estimated to be 5-6 degree (Fig. S2). In this case the observed ranges of rotations and the twisting angle showed a concordance of 90%.

Quantitative studies of the motions revealed that in the actively gated state twisting motions were
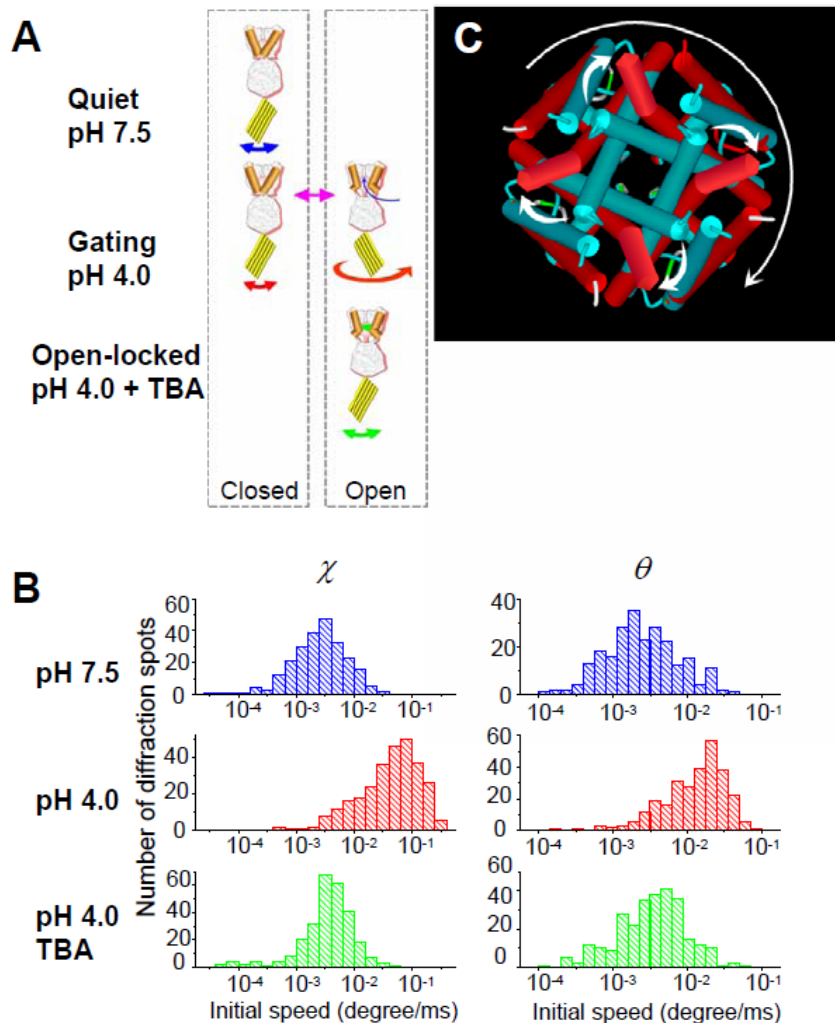
Figure 7. Static and dynamic picture of KcsA channels under various conditions. **A.** Schematic representation of KcsA channel gating under different experimental conditions. The size of the nanocrystal was not scaled relative to that of the channel. **B.** Histograms of the initial speed (Angle/ms = |ΔAngle| / 33 ms) for the full-length KcsA on a logarithmic scale. The left column for the angle χ and the right for the angle θ. **C.** The TM domain of KcsA channel viewed from intracellular side. Blue represents the closed structure and red represents the open structure with a bend of the inner helix. Concerted movements of helices lead to twisting of the channel in a clockwise direction upon opening.

predominant and showed prominent features of gating dynamics. The distributions of the destination angle χ were non-Gaussian (Fig. 3B, 5D) and the MSD curves (Fig. 3C, 5E) were sub-linear. Their characteristics for the full-length and CPD-deleted KcsA channels were common. Closer inspections of the trajectories revealed that runs of consecutive twisting steps in the same direction were prevalent. This behavior suggests a non-random process. Several points might be sampled during a course of a large stride of twisting motions.

To understand the distribution of the twisting angle, first imagine the conformational change between two defined twisting angles. The distribution of the destination angles in clockwise and counter-clockwise twisting can be expected to have two peaks at the symmetrical positions. The absence of such defined peaks and the broad and non-Gaussian distribution shown in this study suggest incomplete tracing of the full conformational pathway partly because of the short lifetimes of spots. The irregular shapes of the histograms may indicate that the bending motions augmented by the flexible CP domain perturbed the traces of the diffraction spots. The S.D.s of the twisting motions from the destination histogram (Fig. 3B, 4C and 5D) should underestimate the real range of twisting. The observed maximum values of twisting angle were ±40 degrees, which may serve as an estimate of the real twisting motion.

To characterize this motion more closely, the angular speeds of the motions, the absolute distance of each step divided by the interval of the video rate, were analyzed. Histograms of the initial angular speeds (the mean of the initial three values of angular speed) for the quiet and blocked conditions were Gaussian (Fig. 7B), indicating dynamic random motions of the channel conformation. In contrast, the initial speeds upon gating were very high and the distributions of the initial angular speeds were extremely skewed or truncated. This can be interpreted to mean that the experimentally determined speeds were only part of the full range of the speed distribution because of the limited time resolution of the experimental system.

What can we draw from the truncated distribution of the speed of χ? The highest speed observed, about 1 degree/ms, may be slower than the expected but not-yet-observed angular speed of conformational changes. It may be the lower extreme of the real motion. Other possibilities remain. It is possible that our observations might be biased. The speed of the motion may be limited by the attached nanocrystal. It has been reported that single molecular measurements of the Fo-F1 complex of proton ATPase revealed rotational motion and its speed increased significantly as the size of labeled substances was reduced (Noji et al., 1997; Yasuda et al., 1998; Yasuda et al., 2001). In this study, the size of the probe was smaller than in previous studies. However, the nanocrystal was flat in shape, and had relatively large rotational inertia. Therefore, the nanocrystal, secured by tight mechanical coupling to the channel with four cysteine residues, may be subject to a large damping force if the initial speed of the motion was very high during the impact of the conformational changes of gating (see Supplemental data, Fig. S7). These dynamic features provide clues on the mechanics of gating motion.

Previous studies of the conformational changes of potassium channels, (Perozo et al., 1998; Perozo et al., 1999; Liu et al., 2001) using EPR measurements revealed changes in the distances between specific residues (residue 116) in the KcsA channel at different pHs. Differences in surface exposure of specifically labeled residues elucidated changes in conformation at different pH for the KcsA channel (Iwamoto et al., 2006; Kelly and Gross, 2003) and other channels (Johnson and Zagotta, 2001; Phillips et al., 2003). This static and local structural information was viewed in our study as an animated movie in the 3D space. Our results reveal that the changes in the distances between helices detected by the previous studies in equilibrium conditions (Kelly and Gross, 2003; Liu et al., 2001; Perozo et al., 1998; Perozo et al., 1999) originate from the twisting motions of the channel. Blunck *et al*. (Blunck et al., 2006) found discrepancies between signals of conformational changes in the inner helix and on and off of single channel currents. It was suggested that fast gating of single channel currents represents gating of the selectivity filter (Blunck et al., 2006; Cordero-Morales et al., 2006), and that the gating of the inner helix was relatively slow. It is likely that in this study we detected the slow gating motions accompanying the motions of inner helix. Although the observed twisting motions were very slow compared to the transition times for the single channel currents, the slowness of these motions does not imply that transitions between the on and off states of the channel current took a long time. Alternatively, stepwise current transitions may appear en route of the twisting motions.

Conclusion
We describe a twisting motion of KcsA channel upon gating. For the channel to be conducting, it has been proposed that the gating helix bends at a glycine hinge in the middle of the M2 helix. In symmetric potassium channels this motion should be concerted among tetrameric subunits and be translated to a rotational motion around the longitudinal axis of the

12

channel. As shown in Fig. 7C clockwise rotation viewed from the cytoplasmic side corresponds to the bending of the gating helices, leading to the open state. The origin of the twisting motion was traced back to the transmembrane domain, because the rotational motion was detected for the CPD-deleted channel and this movement was stopped by TBA.

The dynamic picture of the gating motion obtained in this study provides insight into mechanistic features of conformational changes during gating.

Experimental Procedures

KcsA channel. Purification and mutation procedures for the KcsA channel were described elsewhere (Iwamoto et al., 2006). 1% n-Dodecyl-β-D-maltoside (DDM; Dojindo, Kumamoto, Japan) was used as a detergent. KcsA channels were fixed onto a glass plate in three different orientations: upright, upside-down and sideways. The orientation of the channels on the glass plate was governed through a specific reaction between lysine residues introduced into the KcsA channels and a surface modifying reagent, succinimidyl 6-(3'-(2-pyridyldithio) propionamido) hexanoate (LC-SPDP, PIERCE., Rockford, IL). To fix the channels in the upright position for either the erect or upside-down orientation, two lysine residues in the wild type KcsA channel were replaced by arginine (K14R and K131R). R52 in the extracellular loop was mutated to lysine for the upside-down channel (R52K) and a lysine residue was introduced at 161 site for the erect channel (161K). For the channels laid sideways, the inherent lysine residue (K14) was used to fix the channel. Gold nanocrystals were attached to the channel through the introduced cysteine residues (the wild-type channel lacks cysteine residues). For the upside-down channels and the channels laid sideways a cysteine residue was introduced at the C-terminal end (161C) and for the erect channel a cysteine was introduced in the extracellular loop at site 52 (K52C). Single-channel currents were recorded from the mutated KcsA channels in a planar lipid bilayer (Iwamoto et al., 2006). KcsA channels with the cytoplasmic domain deleted were obtained by chymotrypsin digestion followed by gel-filtrated purification (Doyle et al., 1998).

Atomic force microscopy measurements. KcsA channels (R52K) were fixed upright (upside-down) on an LC-SPDP modified plate and the profiles of heights from the flat surface were examined by AFM (SPA400/SPI3800N, SII NanoTechnology Inc., Chiba, Japan) in solution (Fig. 1B, S1). The heights of the molecule were analyzed from the AFM images using a software package (Scanning Probe Image Processor, SPIP, Image Metrology A/S).

Diffracted X-ray tracking. A glass surface (7 mm × 7 mm) was coated with chromium (4 nm) and gold (thickness 10 nm) and then treated by LC-SPDP. The KcsA channels were fixed by the lysine residues with LC-SPDP. One-dimensional (layer-by-layer) gold nanocrystals grown epitaxially on a NaCl substrate (Sasaki et al., 2001) (Fig. S3) were attached to the KcsA channel by way of the mutated cysteine residues. The electrolyte solution (200 mM KCl buffered with 10 mM Hepes for pH 7.5 or succinic acid for pH 4), including 0.06% (1.2 mM) DDM (the critical micelle concentration = 0.17 mM), was layered on the glass plate at a thickness of 7 μm and covered with a polyimide sheet (Kapton, DuPont). Temperature was strictly controlled at 18°C with CryojetHT (Oxford Instruments., Oxfordshier, UK).

White X-rays (the energy rage: 6 - 30 keV; the beamline BL44B2, SPring-8, Japan) were irradiated as a pulse train for 3.8 s with the pulse duration of 10 ms and an interval of 23 ms. Diffraction spots were recorded by a CCD camera through an X-ray image intensifier (Okumura et al., 2004) at a video rate (30 frames/s). The cross section of the beam was 0.1 mm × 0.1 mm. This procedure was repeated at different positions on a plate automatically (Automatic DXT Measurement System, CHUO ELECTRIC WORKS, Osaka, Japan), and more than 100 image files were obtained from a single glass plate.

The trajectories of diffraction spots on the image plane were traced by software (Image Tracker PTV, NVS). More than 300 spots (except for the erect channel) were collected for each experimental condition. Analyses were performed with Mathematica software (Wolfram Research, Inc., Champaign, IL).

Mean square displacement curves. For each trajectory of a spot, the initially appeared time and position (in χ and θ angles) were defined as a starting time and position. Then the displacement of angles (χ and θ) from the starting position was plotted as a function of time elapsed from the starting time (time lag). The squared displacements as a function of time lag were ensemble averaged to produce the MSD curves. MSD curves, thus obtained, for χ and θ angles were fitted by an exponential function (Thomas, 1986).

$$\langle \chi(t)^2 \rangle = -A \times (1 - \exp[-t/\tau])$$
$$\langle \theta(t)^2 \rangle = -A \times (1 - \exp[-t/\tau])$$

$$D_{rot} = \frac{A}{2\tau}$$

$$D_{tilt} = \frac{A}{4\tau}$$

where D is the diffusion coefficient, t is time, τ is the time constant and A is an amplitude factor.

References

Blunck, R., Cordero-Morales, J. F., Cuello, L. G., Perozo, E., and Bezanilla, F. (2006). Detection of the opening of the bundle crossing in KcsA with fluorescence lifetime spectroscopy reveals the existence of two gates for ion conduction. J. Gen. Physiol. *128*, 569-581.

Bragg, W. H., and Bragg, W. L. (1913). The reflection of x-rays by crystals. Proc. Roy. Soc. *88A*, 428-438.

Cordero-Morales, J. F., Cuello, L. G., Zhao, Y., Jogini, V., Cortes, D. M., Roux, B., and Perozo, E. (2006). Molecular determinants of gating at the potassium-channel selectivity filter. Nat. Struct. Mol. Biol. *13*, 311-318.

Cortes, D. M., Cuello, L. G., and Perozo, E. (2001). Molecular architecture of full-length KcsA: role of cytoplasmic domains in ion permeation and activation gating. J. Gen. Physiol. *117*, 165-180.

Doyle, D. A., Morais Cabral, J., Pfuetzner, R. A., Kuo, A., Gulbis, J. M., Cohen, S. L., Chait, B. T., and MacKinnon, R. (1998). The structure of the potassium channel: molecular basis of K^+ conduction and selectivity. Science *280*, 69-77.

Faraldo-Gomez, J. D., Kutluay, E., Jogini, V., Zhao, Y., Heginbotham, L., and Roux, B. (2007). Mechanism of intracellular block of the KcsA K^+ channel by tetrabutylammonium: insights from X-ray crystallography, electrophysiology and replica-exchange molecular dynamics simulations. J. Mol. Biol. *365*, 649-662.

Friedrich, W., Knipping, P., and Laue, M. V. (1912). Interferenz-erscheinungen bei rontgenstrahlen. Proc. Bavarian Acad. Sci., 303-322.

Heginbotham, L., LeMasurier, M., Kolmakova-Partensky, L., and Miller, C. (1999). Single streptomyces lividans K^+ channels: functional asymmetries and sidedness of proton activation. J. Gen. Physiol. *114*, 551-560.

Hille, B. (2001). Ion channels of excitable membranes, 3rd edn. (Sunderland, MA, Sinauer Associates).

Iwamoto, M., Shimizu, H., Inoue, F., Konno, T., Sasaki, Y. C., and Oiki, S. (2006). Surface structure and its dynamic rearrangements of the KcsA potassium channel upon gating and tetrabutylammonium blocking. J. Biol. Chem. *281*, 28379-28386.

Jiang, Y., Lee, A., Chen, J., Cadene, M., Chait, B. T., and MacKinnon, R. (2002). Crystal structure and mechanism of a calcium-gated potassium channel. Nature *417*, 515-522.

Jiang, Y., Lee, A., Chen, J., Ruta, V., Cadene, M., Chait, B. T., and MacKinnon, R. (2003). X-ray structure of a voltage-dependent K^+ channel. Nature *423*, 33-41.

Johnson, J. P., Jr., and Zagotta, W. N. (2001). Rotational movement during cyclic nucleotide-gated channel opening. Nature *412*, 917-921.

Kelly, B. L., and Gross, A. (2003). Potassium channel gating observed with site-directed mass tagging. Nat. Struct. Biol. *10*, 280-284.

Kuo, A., Gulbis, J. M., Antcliff, J. F., Rahman, T., Lowe, E. D., Zimmer, J., Cuthbertson, J., Ashcroft, F. M., Ezaki, T., and Doyle, D. A. (2003). Crystal structure of the potassium channel KirBac1.1 in the closed state. Science *300*, 1922-1926.

LeMasurier, M., Heginbotham, L., and Miller, C. (2001). KcsA: it's a potassium channel. J. Gen. Physiol. *118*, 303-314.

Lenaeus, M. J., Vamvouka, M., Focia, P. J., and Gross, A. (2005). Structural basis of TEA blockade in a model potassium channel. Nat. Struct. Mol. Biol. *12*, 454-459.

Liu, Y. S., Sompornpisut, P., and Perozo, E. (2001). Structure of the KcsA channel intracellular gate in the open state. Nat. Struct. Biol. *8*, 883-887.

Long, S. B., Campbell, E. B., and Mackinnon, R. (2005). Crystal structure of a mammalian voltage-dependent Shaker family K^+ channel. Science *309*, 897-903.

Noji, H., Yasuda, R., Yoshida, M., and Kinosita, K., Jr. (1997). Direct observation of the rotation of F1-ATPase. Nature *386*, 299-302.

Okumura, Y., Miyazaki, T., Taniguchi, Y., and Sasaki, Y. C. (2005). Fabrications of dispersive gold one-dimensional nanocrystals. Thin Solid Films *471*, 91-95.

Okumura, Y., Oka, T., Kataoka, M., Taniguchi, Y., and Sasaki, Y. C. (2004). Picometer-scale dynamical observations of individual membrane proteins: the case of bacteriorhodopsin. Phys. Rev. E Stat. Nonlin. Soft Matter Phys. *70*, 021917.

Perozo, E., Cortes, D. M., and Cuello, L. G. (1998). Three-dimensional architecture and gating mechanism of a K^+ channel studied by EPR spectroscopy. Nat. Struct. Biol. *5*, 459-469.

Perozo, E., Cortes, D. M., and Cuello, L. G. (1999). Structural rearrangements underlying K^+-channel activation gating. Science *285*, 73-78.

Phillips, L. R., Enkvetchakul, D., and Nichols, C. G. (2003). Gating dependence of inner pore access in inward rectifier K$^+$ channels. Neuron *37*, 953-962.

Sasaki, Y. C., Okumura, Y., Adachi, S., Suda, H., Taniguchi, Y., and Yagi, N. (2001). Picometer-scale dynamical x-ray imaging of single DNA molecules. Phys. Rev. Lett. *87*, 248102.

Sasaki, Y. C., Suzuki, Y., Yagi, N., Adachi, S., Ishibashi, M., Suda, H., Toyota, K., and Yanagihara, M. (2000). Tracking of individual nanocrystals using diffracted x rays. Phys. Rev. E Stat. Phys. Plasmas. Fluids Relat. Interdiscip. Topics *62*, 3843-3847.

Schrempf, H., Schmidt, O., Kummerlen, R., Hinnah, S., Muller, D., Betzler, M., Steinkamp, T., and Wagner, R. (1995). A prokaryotic potassium ion channel with two predicted transmembrane segments from *Streptomyces lividans*. EMBO J. *14*, 5170-5178.

Sigg, D., and Bezanilla, F. (2003). A physical model of potassium channel activation: from energy landscape to gating kinetics. Biophys. J. *84*, 3703-3716.

Sigg, D., Bezanilla, F., and Stefani, E. (2003). Fast gating in the Shaker K$^+$ channel and the energy landscape of activation. Proc. Natl. Acad. Sci. U.S.A. *100*, 7611-7615.

Terada, T. (1913a). On the transmittion of x-rays through crystals. Proc. Tokyo Math.-Phys. Soc. *7*, 60-70.

Terada, T. (1913b). X-rays and crystals. Nature *91*, 135-136.

Terada, T. (1913c). X-rays and crystals. Nature *91*, 213.

Thomas, D. D. in *Techniques for the analysis of membrane proteins* C. I. Ragan, R. J. Cherry, Eds. (Chapman and Hall, London, 1986

VanAken, T., Foxall-Vanaken, S., Castleman, S., and Ferguson-Miller, S. (1986) Alkyl Glycoside Detergents: Synthesis and Applications to the Study of Membrane Proteins. Methods in Enzymol. *125*, 27-35.

Webster, S. M., Del Camino, D., Dekker, J. P., and Yellen, G. (2004). Intracellular gate opening in Shaker K$^+$ channels defined by high-affinity metal bridges. Nature *428*, 864-868.

Yasuda, R., Noji, H., Kinosita, K., Jr., and Yoshida, M. (1998). F1-ATPase is a highly efficient molecular motor that rotates with discrete 120 degree steps. Cell *93*, 1117-1124.

Yasuda, R., Noji, H., Yoshida, M., Kinosita, K., Jr., and Itoh, H. (2001). Resolution of distinct rotational substeps by submillisecond kinetic analysis of F1-ATPase. Nature *410*, 898-904.

Zhou, M., Morais-Cabral, J. H., Mann, S., and MacKinnon, R. (2001a). Potassium channel receptor site for the inactivation gate and quaternary amine inhibitors. Nature *411*, 657-661.

Zhou, Y., Morais-Cabral, J. H., Kaufman, A., and MacKinnon, R. (2001b). Chemistry of ion coordination and hydration revealed by a K$^+$ channel-Fab complex at 2.0 A resolution. Nature *414*, 43-48.

Zimmer, J., Doyle, D. A., and Grossmann, J. G. (2006). Structural characterization and pH-induced conformational transition of full-length KcsA. Biophys. J. *90*, 1752-1766.